

## Application of Wiener and Adaptive Filters to GPS and Glonass Data from the Rapid Prototyping Array

Geoffrey C. Bower

### ABSTRACT

Wiener and adaptive filters can be used to cancel radio frequency interference through the use of reference antenna observations. We discuss the basic theory of these filters, their relationship to other techniques, and the application of these filters to GPS and Glonass data obtained at the Rapid Prototyping Array. We achieve a maximum rejection of 30 dB. We also discuss potential implementation of these techniques for the Allen Telescope Array. We end with a list of unresolved issues and experiments that address those issues.

### 1. Adaptive Filters

Cancellation using adaptive filters is a potential RFI mitigation technique for the Allen Telescope Array. These algorithms operate on the sampled voltages of either each antenna or the output of a beamformer through the use of finite impulse response (FIR) filters. These techniques rely on independent measurements of the interferer through a reference antenna but they do not require knowledge of the location of the interferer beyond a primary beam width or any of its other properties. The properties of adaptive filter techniques have been discussed in detail by Barnbaum & Bradley (1998) and Vaseghi (2000).

These filters can also be made to operate in the frequency domain on autocorrelation and cross-correlation power spectra. This is known as post-correlation interference excision (Briggs, Bell & Kesteven 2000). These techniques are also closely related to parametric estimation techniques which exploit known properties of the interferer along with reference measurements to create a noise free model of the interferer (Ellingson, Bunton & Bell 2001).

The optimal solution to the filter problem is known as the Wiener solution. This minimizes with a least-squares method the power of the difference between a measurement of the interferer and a measurement of the source which is corrupted by the interferer. For a reference signal  $r(t_i)$  and a primary signal  $p(t_i)$ , the error signal is

$$e(t_i) = p(t_i) - \mathbf{R}w, \tag{1}$$

where  $\mathbf{R}$  is a matrix composed of  $q$  delayed vectors of  $r(t_i)$  and  $w$ , the filter, is a vector of length  $q$ . The multiplication is the equivalent of the convolution of  $r(t_i)$  with  $w$ . The Wiener solution is

the vector  $w$  that minimizes  $e^2$ :

$$w = \mathbf{X}_{r,r}^{-1} x_{p,r}. \quad (2)$$

$\mathbf{X}_{r,r}^{-1}$  is an autocorrelation matrix of the delayed vectors  $r$ .  $x_{p,r}$  is the cross-correlation vector between the primary and reference signals over  $q$  delays. This formalism can be generalized so that averages are used to form the correlation matrices and vectors.

In some cases, the Wiener solution may be too expensive computationally. A popular approximation applied is the least mean square (LMS) filter. This filter estimates the subsequent filter based on the error  $e$ :

$$w(m+1) = w(m) + \mu p e. \quad (3)$$

The parameter  $\mu$  determines how rapidly the approximation converges on the Wiener solution. If it is too large, the solutions blow up. Too small, and the solutions don't approach the optimal solution.

The Wiener filter can be generalized to the case of multiple reference sources. In this case, the error signal is

$$e(t_i) = p(t_i) - \sum_{k=1}^N \mathbf{R}_k w_k, \quad (4)$$

where  $\mathbf{R}_k$  is the matrix  $\mathbf{R}$  for the  $k$ th reference source. Then, the Wiener solution is defined by

$$x_{p,i} = \sum_{k=1}^N w_k^T \mathbf{X}_{k,i}. \quad (5)$$

Here,  $\mathbf{X}_{k,i}$  is the cross-correlation matrix of the  $k$  and  $i$  reference signals and  $x_{p,i}$  is the cross-correlation lag spectrum between the primary signal and the  $i$  reference signal. The solution for  $w_k$  can be rewritten as a matrix problem in which one must invert a matrix that is  $N * q$ -square. This multiple reference solution is particularly useful for the application of dual-polarization signals but also holds for multiple independent interferers. In the special case of two interferers, the solution for  $w_k$  is

$$w_1 = (x_{p,1} - x_{p,2} \mathbf{X}_{2,2}^{-1} \mathbf{X}_{2,1}) \left( \mathbf{X}_{1,1} - \mathbf{X}_{1,2} \mathbf{X}_{2,2}^{-1} \mathbf{X}_{2,1} \right)^{-1}, \quad (6)$$

$$w_2 = (x_{p,2} - x_{p,1} \mathbf{X}_{1,1}^{-1} \mathbf{X}_{1,2}) \left( \mathbf{X}_{2,2} - \mathbf{X}_{2,1} \mathbf{X}_{1,1}^{-1} \mathbf{X}_{1,2} \right)^{-1}. \quad (7)$$

### 1.1. Relationship of Nulling and Pre- and Post-correlation Techniques

A number of important techniques for interference mitigation are closely related. We demonstrate those relationships here. For a correlation matrix  $\mathbf{X} = s_1 s_2^H$  for two time series  $s_1$  and  $s_2$ , we can write

$$\mathbf{X} = \mathbf{X}_v + \sigma_a^2 a a^H + \sigma^2 \mathbf{I}. \quad (8)$$

$\mathbf{X}_v$  is the visibility information due to astronomical source structure. The vector  $a$  is the direction vector for an interferer of power  $\sigma_a^2$ . The last term is noise power in the measurement.

Nulling can be understood as the application of a projection matrix  $\mathbf{P}_a^\perp$  to  $\mathbf{X}$  (Leshem, van der Veen & Boonstra 2000). The resulting matrix is

$$\mathbf{X}' = \mathbf{P}_a^\perp \mathbf{X} \mathbf{P}_a^\perp = \mathbf{P}_a^\perp \mathbf{X}_v \mathbf{P}_a^\perp + \sigma^2 \mathbf{P}_a^\perp \mathbf{P}_a^\perp. \quad (9)$$

Importantly, the result is independent of  $\sigma_a$  and  $a$ .

Cancellation can be shown to be a similar matrix operation. In the post-correlation domain, subtraction of a matrix  $\sigma_a^2 aa^H$  from  $\mathbf{X}$  is the same as two-sided multiplication of  $\mathbf{X}$  by  $\mathbf{C} = \mathbf{I} - \alpha uu^H$ . Note that since this cancellation is applied to the correlation matrix it is not the same time-series operation we described in the first Section.

However, we can also show that pre- and post-correlation techniques are intimately related. If we apply the matrices before correlation, then the results are identical to post-correlation:

$$\mathbf{X}' = \mathbf{P} \mathbf{X} \mathbf{P} = (\mathbf{P} s_1) (s_2^H \mathbf{P}). \quad (10)$$

For  $\mathbf{P} = \mathbf{C}$ ,

$$\mathbf{X}' = (s_1 - \alpha uu^H s_1) (s_2^H - \alpha s_2^H uu^H). \quad (11)$$

That is, the result can be achieved through subtraction of a vector from the original time series data. The vector  $u$  contains the reference antenna signal, which is cross-correlated with  $s_1$ .

## 2. The GPS and Glonass Data

Several GPS and Glonass data sets were obtained. A typical data set of each type is described below. CD-ROMs of all data sets are available on request. Further description is available at <http://astro.berkeley.edu/~gbower/rfi>.

The Glonass and GPS data are similar in type. They both produce spread spectrum signals, the Glonass from FDMA and the GPS from CDMA. The C/A code for the two are 0.5 Mbits/sec and 1.0 Mbits/sec, respectively. These repeat every 1 millisecond. The P code for the two are 5 Mbits/sec and 10 Mbits/sec, respectively. These repeat in 1 second and on a timescale of many days, respectively.

### 2.1. Sample GPS Data

The Rapid Prototype Array observed the Navstar/GPS satellite #35 on 10 April 2001. Two line element (TLE) data were taken from the Orbital Information Group at NASA (<http://oig1.gsfc.nasa.gov>). The TLE used, which was updated on 8 April 2001, is

NAVSTAR 35 (USA 96)

```
1 22877U 93068A 01098.67728172 -.00000077 +00000-0 +00000-0 0 02011
2 22877 055.8300 339.4467 0056503 332.8560 026.8958 02.00564138054625
```

Other Navstar/GPS satellites above the horizon at the time of observation were numbers 15, 23, 32, 33, 34, 36, 38 and 39.

Data were obtained at 17:58 UT 10 April 2001. The expected location of the satellite at the RPA site was azimuth 68.7 deg, elevation 57.8 deg. Six antennas were used. Antenna one was pointed to put the satellite in the main beam. Antennas two through six were pointed to put the satellite at azimuth 68 and elevation 66.

The data-taking was triggered with a rapidly rising edge to the A/D converter. The data are synchronized to approximately 100 nsec. No compensation was made for geometric or instrumental delays.

Data were obtained in two polarizations for each antenna with 30 Msamples/sec sampling. Sample bytes were 8-bits in length. Zero voltage corresponds to approximately 127.5 counts.

Local oscillators were set so that 1575.42 MHz was mixed to 7.5 MHz before sampling. A 10 MHz IF passband filter sets the usable range of the band from 1570 to 1580 MHz, roughly.

## 2.2. Glonass Data

Observations of the Glonass 82 satellite were obtained at 18:47 UT on 21 June 01. The TLE for the satellite at the time was:

GLONASS 82 (779)

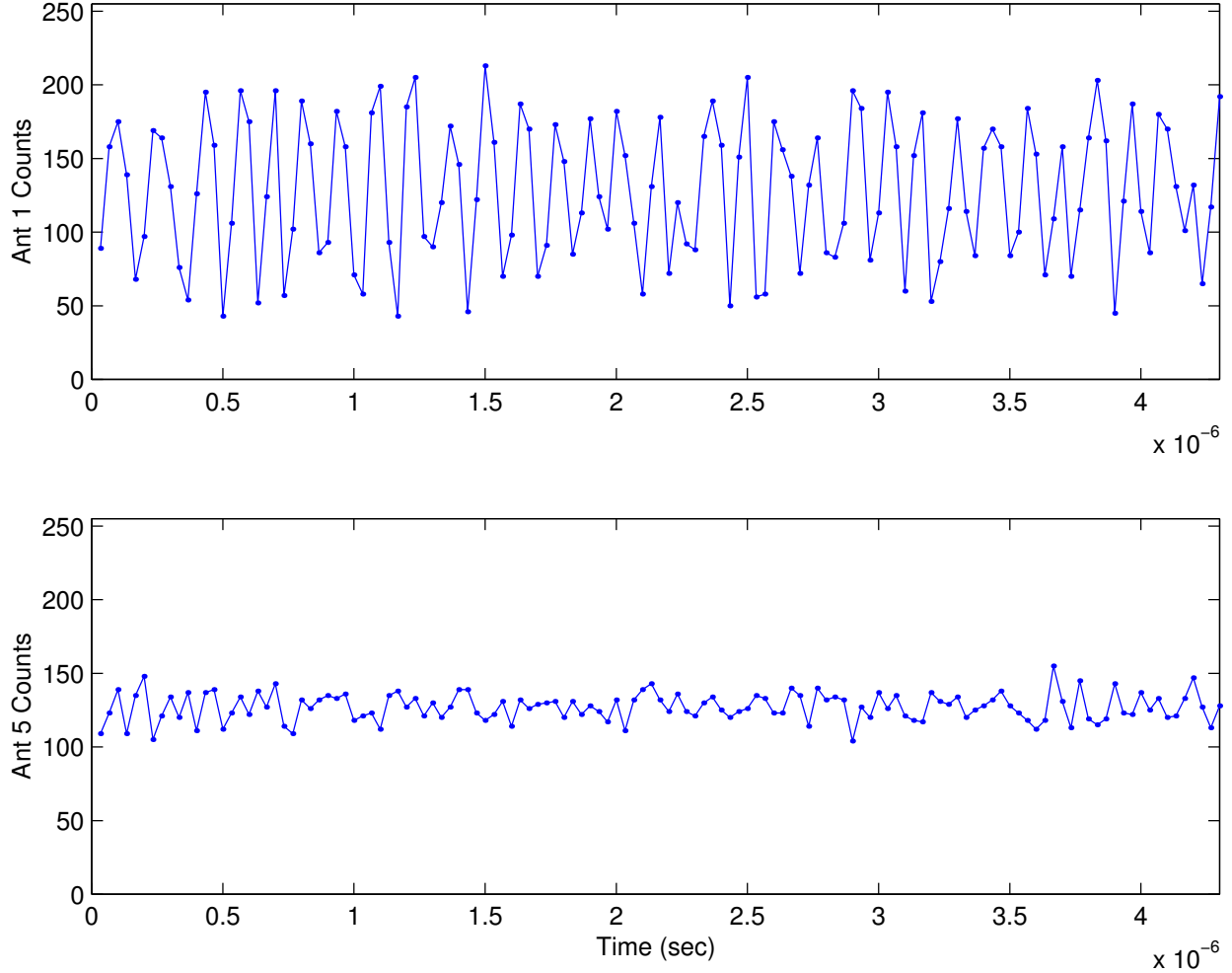
```
1 25593U 98077A 01171.46971065 -.00000030 00000-0 10000-3 0 6842
2 25593 65.1248 21.8324 0013211 71.1204 65.8034 2.13101993 19224
```

The satellite was located at azimuth 344 deg and elevation 68 deg. We put the satellite in the main beam of antenna 1 and at azimuth offsets of +4 degrees for antennas 2 and 3, +8 degrees for antennas 4 and 5, and +12 degrees for antennas for antennas 6 and 7.

The data were obtained in standard dual polarization mode. A total of 255 x 256 x 1024 samples were obtained in each polarization at a sample rate of 30 Msamples/sec. The sky frequency was 1603 MHz.

Additionally, noise data were taken with the same azimuth positions and an elevation offset of -15 degrees. A total of 256 x 1024 samples were obtained in each polarization.

Fig. 1.— Time series data for two antennas. Counts are proportional to voltage.



### 3. Analysis of the Data & Application of the Filter

In Figure 1 we show a short segment of the time series data for two antennas. The GPS signal dominates the noise for antenna 1, which had the GPS satellite in its main beam. The GPS signal is comparable to the noise for antenna 5, which was offset by 8 degrees.

The filter was applied first to the two polarizations of antenna 1. The channel 0 data were used as the reference signal and the channel 1 data were used as the primary signal. A substantial fraction of the GPS signal was eliminated through the use of the filter. Figure 2 shows the time series, filter and before and after spectra after operation on 8 msec of data. The filter was also applied with channel 0 of antenna 1 as reference and channel 0 of antenna 2 as primary (Figure 3).

### 3.1. Long Integrations and Dual Polarization Filters

We applied updated Wiener filters successively to the time series data. The filters were determined and applied on a timescale  $\tau_i$  over an interval  $\tau_0 = N * \tau_i$ . We used both single polarization and dual polarization reference signals to eliminate the interference.

In Figure 4 we see that the dual polarization mode is more successful in eliminating the interference. The rms residual in the power spectrum after 2 seconds of integration is -26 dB down from the original rms noise and several dB down from that found with a single polarization reference source. Using a short integration on blank sky, we also see that the method produces residuals that are close to that expected in the absence of the GPS signal.

Similar results are found for Glonass (Figure 5). We achieved -30 dB RFI rejection with the dual polarization mode, an improvement with dual polarization mode over single polarization mode and near noise-limited performance. In this case, we also find that the rms residual decreases as  $t^{-1/2}$  to our longest integration time. This level of rejection is comparable to that reported for the parametric estimation technique (Ellingson *et al.* 2001).

In many instances with this technique, though, we found that the performance saturated after achieving a certain level of rejection. We were able to increase the attenuation with a model of the bandpass shape. However, we suspect that this continues to limit our ability to assess the performance of this technique. For future experiments, an adequate measurement of the bandpass shape is crucial.

### 3.2. Phased Array Application

We discuss in Section 4 the advantages of implementing a Wiener filter on the output of a phased array signal rather than on the output of each antenna signal. Here, we discuss the results of simulating a phased array output using Glonass and GPS data. We summed together a single polarization signal from three antennas with a GPS signal and three antennas with a Glonass signal. We used both polarizations of the reference signals for GPS and Glonass. The filter weights indicate that we are sensitive to multiple delays for each reference signal (Figure 6). We achieve -25 dB rejection of the total signal (Figure 7). It is unclear whether the measured asymptote in rms is due to irregular bandpass shapes or imperfect rejection.

### 3.3. Necessary Timescale for Filter Computation

We typically computed the Wiener filter for  $16 \times 1024$  samples, or once every 0.491 msec. We did not find substantial change with longer integration periods. There was degradation with shorter integration periods, indicative of a lack of INR.

Surprisingly, we found that it was not necessary to update the filter components frequently. We compared the effect of no updates to the filter after its first calculation to updates every integration period (Figures 8 and 9). In the case of Glonass, we saw no difference up to a few hundred milliseconds. In the case of GPS, we saw no difference up to 2 seconds. This second result may be due to large bandpass irregularities that limit the sensitivity of both calculations.

#### 4. Implementation of an Adaptive Filter in the ATA

A Wiener filter provides a clean voltage to backend systems. This is particularly useful to SETI and pulsar detectors, which process the voltage information. Users of spectrometers and correlators are interested in the statistics of the power spectrum. For these applications, the Wiener filter may be overkill. The post-correlation technique may be a more natural solution.

For use with a beamformer that provides outputs to backend systems, there are two possible implementations of a Wiener filter. In the first case, the modified reference signal is subtracted directly from each antenna’s signal before entering the beamformer. This method would provide output usable by correlators. In the second case, the reference signal is subtracted from the phased array output. Obviously, this method is not applicable to correlators. However, it is substantially simpler in its implementation. For antenna-based cancellation in the current ATA design, at least  $350 \times 2$  FIR filters are necessary. Cross-correlations must be computed for each antenna with each reference antenna, requiring either the use of a large special purpose correlator or substantial resources from the astronomy correlator. Full implementation of the beamformer design requires only a small special purpose correlator and a single FIR filter per beam. This system can be viewed as an independent backend and developed as a stand-alone system.

Important parameters for either implementation are the number of filter taps  $q$ , the precision of the filter weights, and the timescale for the update of the filter  $\tau$ .

The number of filter taps  $q$  is set by the maximum potential delay between the arrival of the interferer and the source signal at the primary antenna  $\tau_{i,s}$  with respect to arrival of the interferer at the reference antenna. In the phased array case,  $\tau_{i,s}$  is the maximum for all antennas. The number of filter taps is

$$q \approx \frac{\tau_{i,s}}{\tau_s}, \quad (12)$$

where  $\tau_s$  is the sample rate. This length must be padded with sufficient filter elements to permit accurate estimation of the signal. This number is on the order of 16, based on our experiments. In the case of a single primary antenna, a reference antenna nearby and no multipath,  $\tau_{i,s}$  is very small. In the case of a 2-D array with maximum baseline  $b$  and no multipath, then  $q \sim b/c/\tau_s$ . For the ATA, with  $b = 0.7$  km,  $\tau_s = 5$  nsec,  $q \approx 500$ . If multipath external to the array is significant, then  $q$  must be increased accordingly.

The timescale for the update of the filter is determined by how rapidly the interferer evolves.

Our experiments with Glonass and GPS indicate that a timescale of 100 msec may be sufficient.

The great difficulty of any implementation is that the output of a correlator is necessary to determine the weights of the filter. The correlator must compute  $q$  lags to match the filter size. This can be eliminated if the LMS solution is accepted.

## 5. Conclusions and Further Work

This document demonstrates that a Wiener filter approach can be used to eliminate Glonass and GPS signals at a level of approximately 30 dB. There is reason to believe that the technique could produce greater attenuation but this has not been demonstrated. The technique appears to be successful for phased array as well as antenna-by-antenna implementation.

There are still a number of unresolved questions regarding the Wiener filter technique:

- What is the ultimate limit in attenuation?
- Can we reduce interference as easily for weak sources as for strong sources?
- How close to the thermal noise limit are we approaching? Under what circumstances does the technique add noise to the data stream?
- Do the required integration and update timescales change with interferer or observing mode?
- What role does an approximate technique like the LMS solution play in a real implementation?
- Are there effects that are baseline dependent?
- Does the technique distort known astronomy signals?
- Does correlated noise leak into the system in the antenna-by-antenna method?
- Does the phased array technique become noise dominated when attempting to determine filter coefficients? This is potentially a substantial problem when phasing together hundreds of antennas.
- Are there other statistics for the evaluation the success of this technique that would be more relevant to SETI or pulsar experiments?

We can address many of these issues with a handful of experiments.

- Application of the technique to Iridium and radar. Iridium has different signal characteristics and moves more rapidly across the sky. Radar behavior is very different from satellite behavior.
- Deeper integrations with improved bandpass removal. This will permit the study of weaker interferers. Tracking of a Glonass signal across the sky for a lengthy period also of time will also

study the effect of changing conditions.

- OH and Glonass experiment. How is the OH signal affected by the removal of the Glonass signal?

Analytical work on the effects of a phased array signal is also necessary.

## 6. References

Barnbaum, C. & Bradley, R.F., 1998, AJ, 115, 2598

Briggs, F.H., Bell, J.F. & Kesteven, 2000, AJ, 120, 3351

Ellingson, S.W., Bunton, J.D. & Bell, J.F., 2001, ApJS, 135, 87

Leshem, A., van der Veen, A.-J. & Boonstra, A.-J., 2000, ApJS, 131, 355

Vaseghi, S.V., 2000, “Advanced Digital Signal Processing and Noise Reduction,” 2nd Ed., Wiley & Sons, New York

Fig. 2.— The application of a Wiener filter to two channels containing GPS signal. In this case, the two channels are orthogonal polarizations on the same antenna. The top panel shows a small subset of the time series voltage of the primary (blue), reference (green) and model (red). The middle panel shows the filter as a function of delay. The primary signal was arbitrarily delayed by 16 samples. The bottom panel shows the primary signal (blue) containing the GPS signal and the cleaned error signal (green).

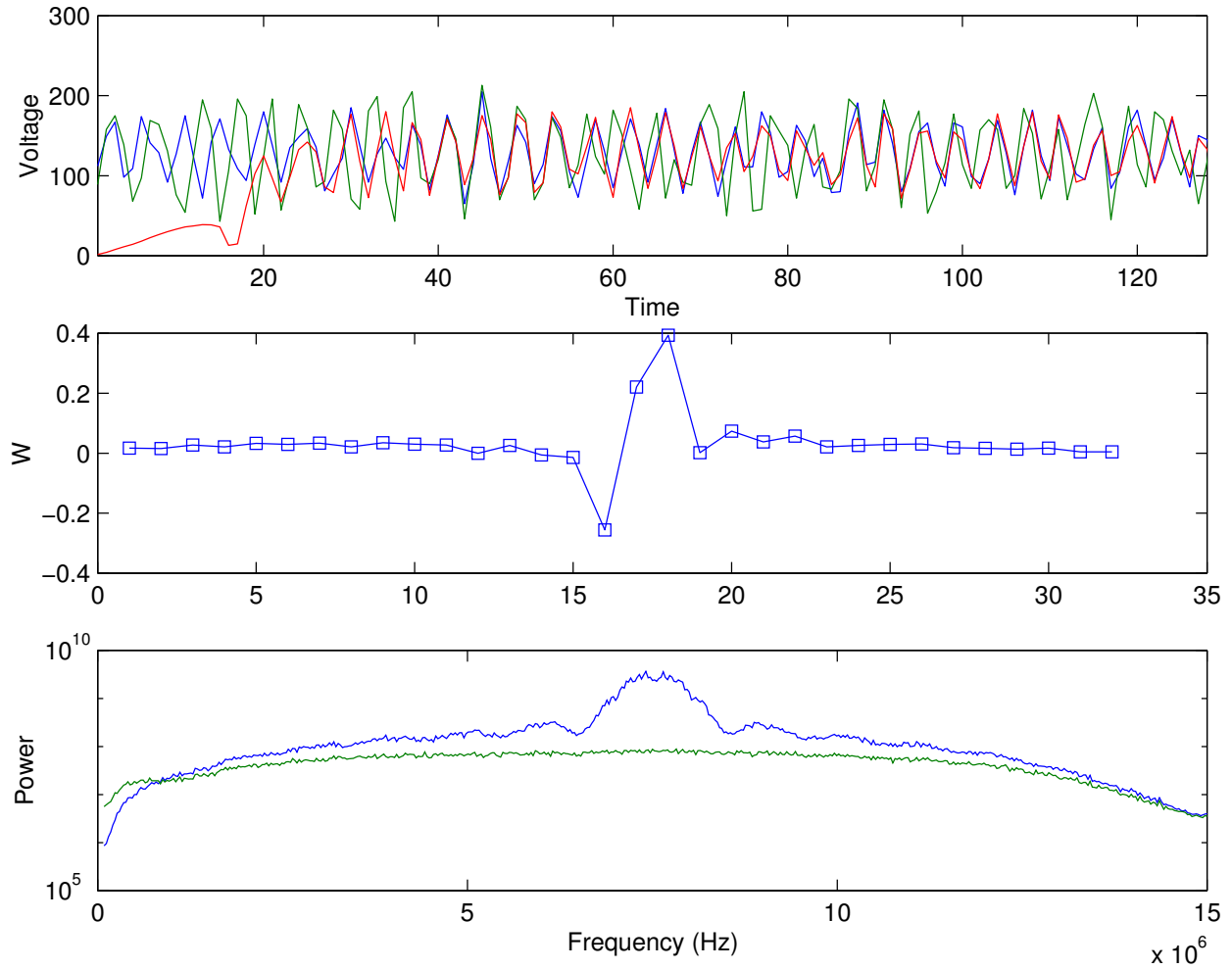


Fig. 3.— The application of a Wiener filter to two channels containing GPS signal. Plots are the same as Figure 2. The reference channel is from antenna 1 and the primary channel is from antenna 2.

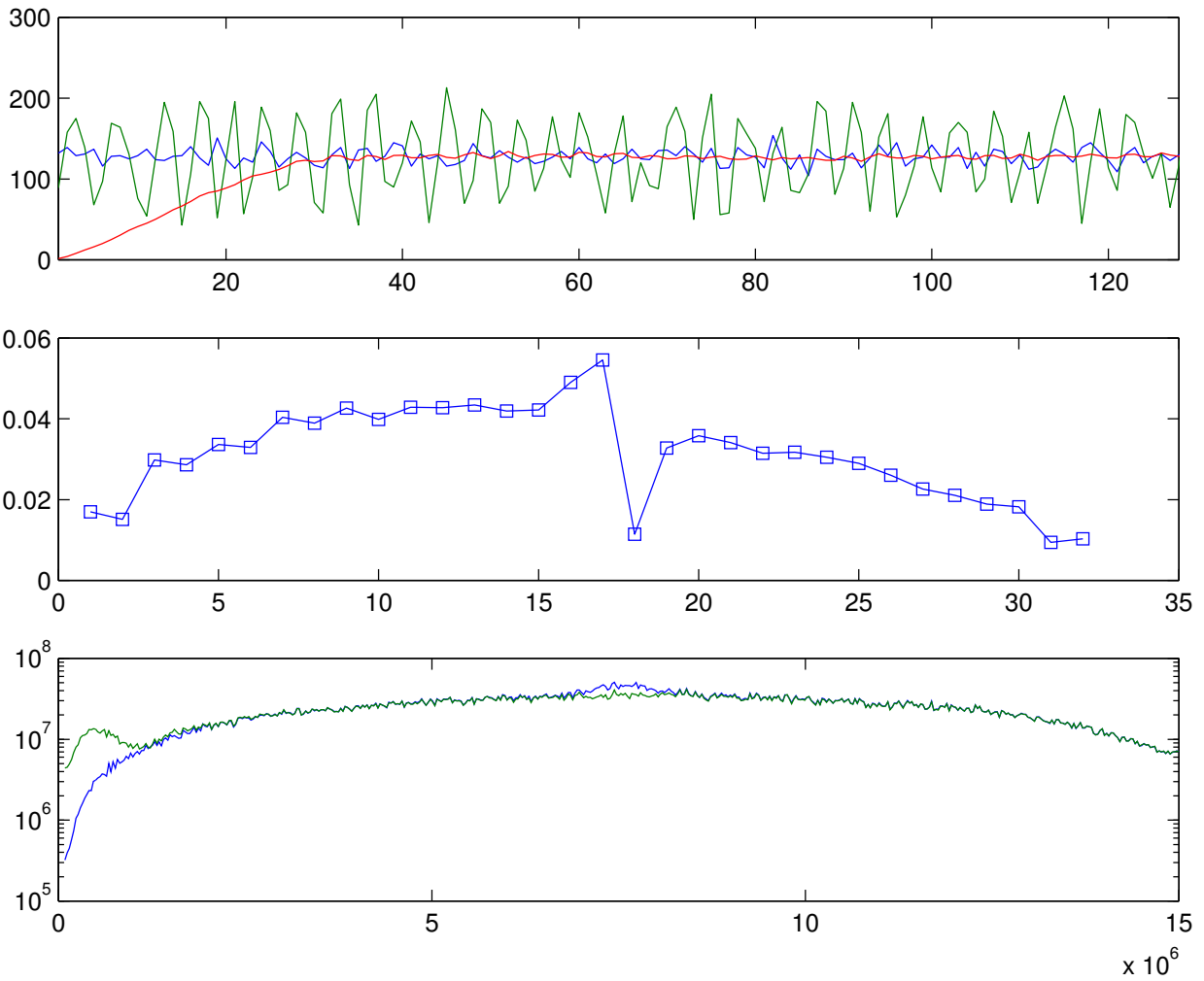


Fig. 4.— The rms as a function of integration time with successive application of Wiener filters to GPS data. In the top panel, we show the power spectrum with and without (blue) removal of the modified reference signal. Results are shown for single (green) and dual (red) polarization modes. In the bottom panel, green crosses indicate the rms residual in the power spectrum from the dual polarization mode. Blue circles indicate the rms residual for the single polarization mode. Purple stars indicate the rms residual for a noise spectrum. The straight red and aqua curves are  $t^{-1/2}$  curves fit to the single and dual polarization residuals, respectively. The gold line is the residual in the uncorrected power spectrum.

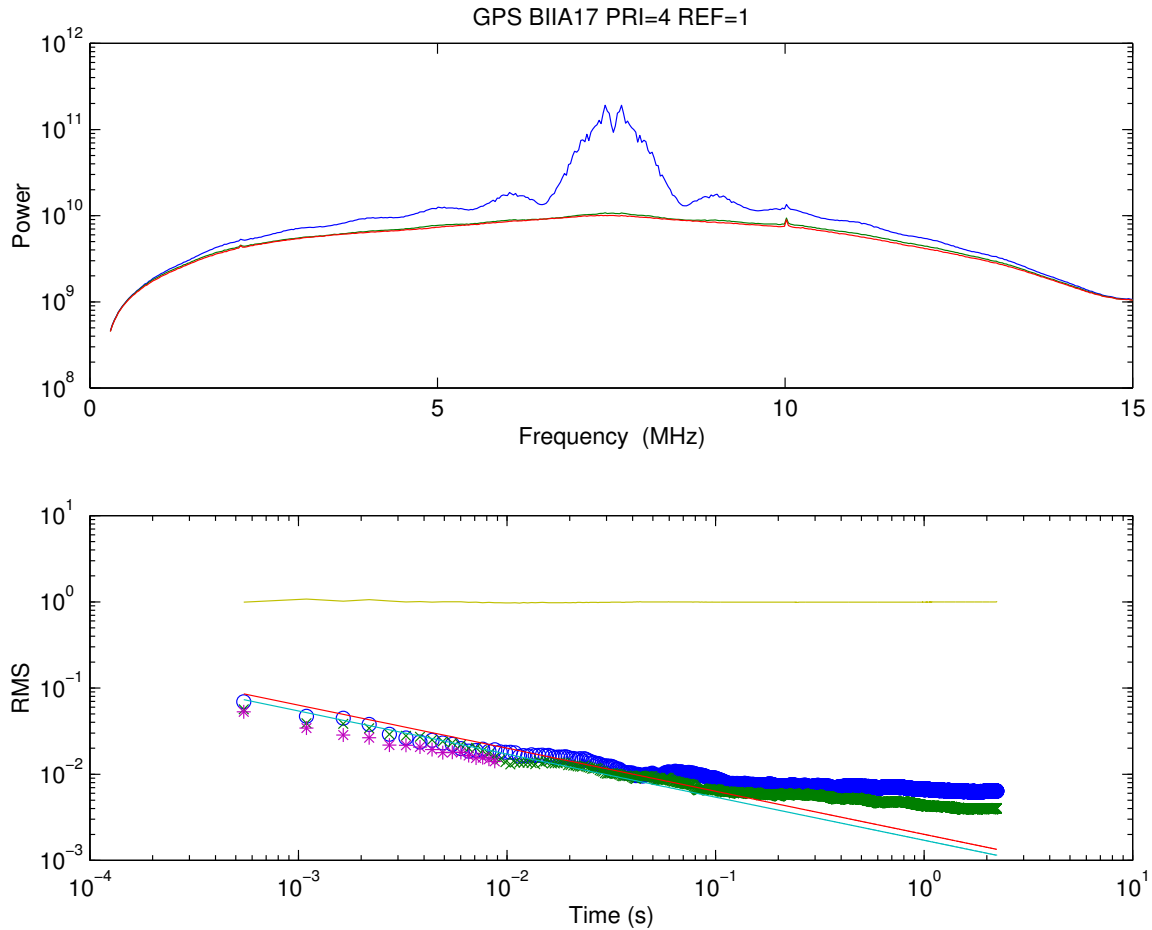


Fig. 5.— The rms as a function of integration time with successive application of Wiener filters to Glonass data. Symbols are the same as in Figure 4.

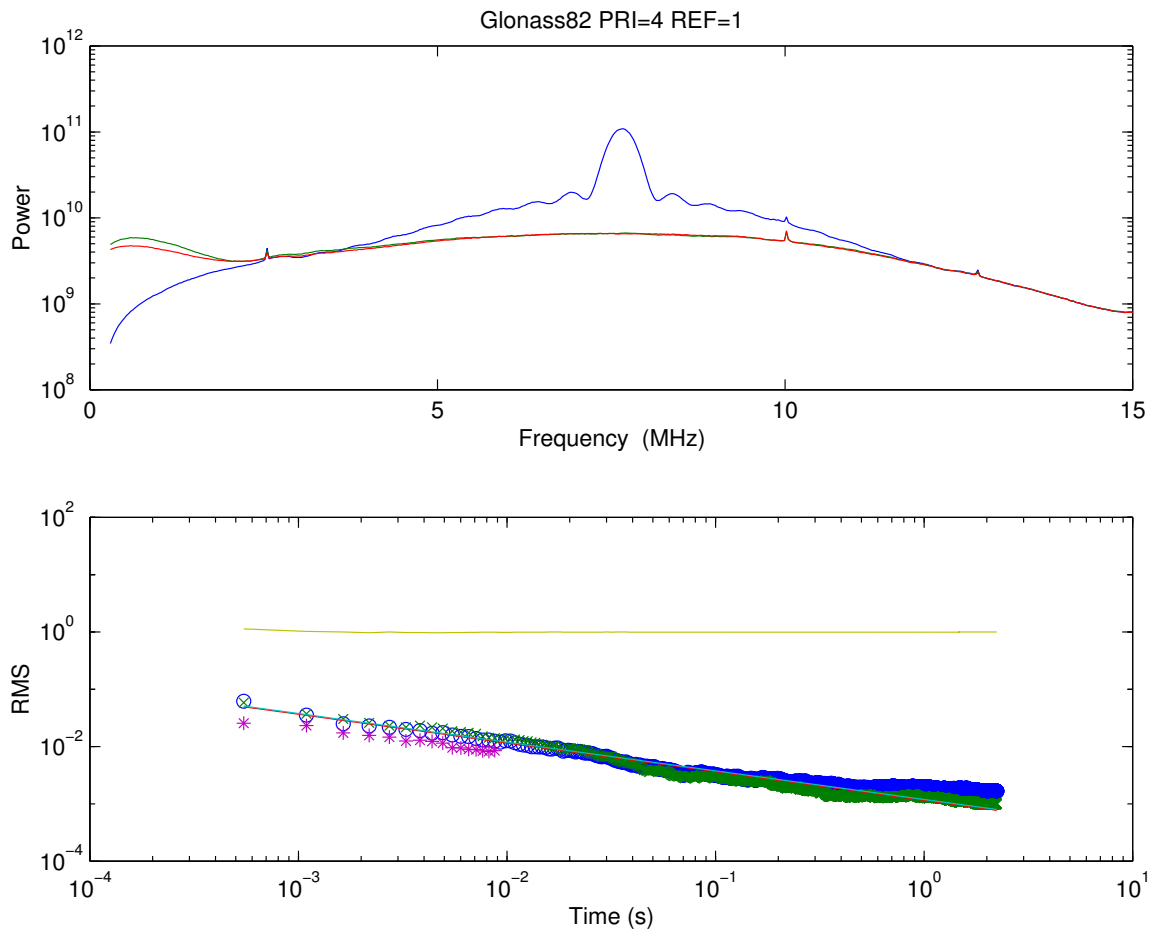


Fig. 6.— Filter weights for phased array with two dual polarization reference signals for GPS and Glonass.

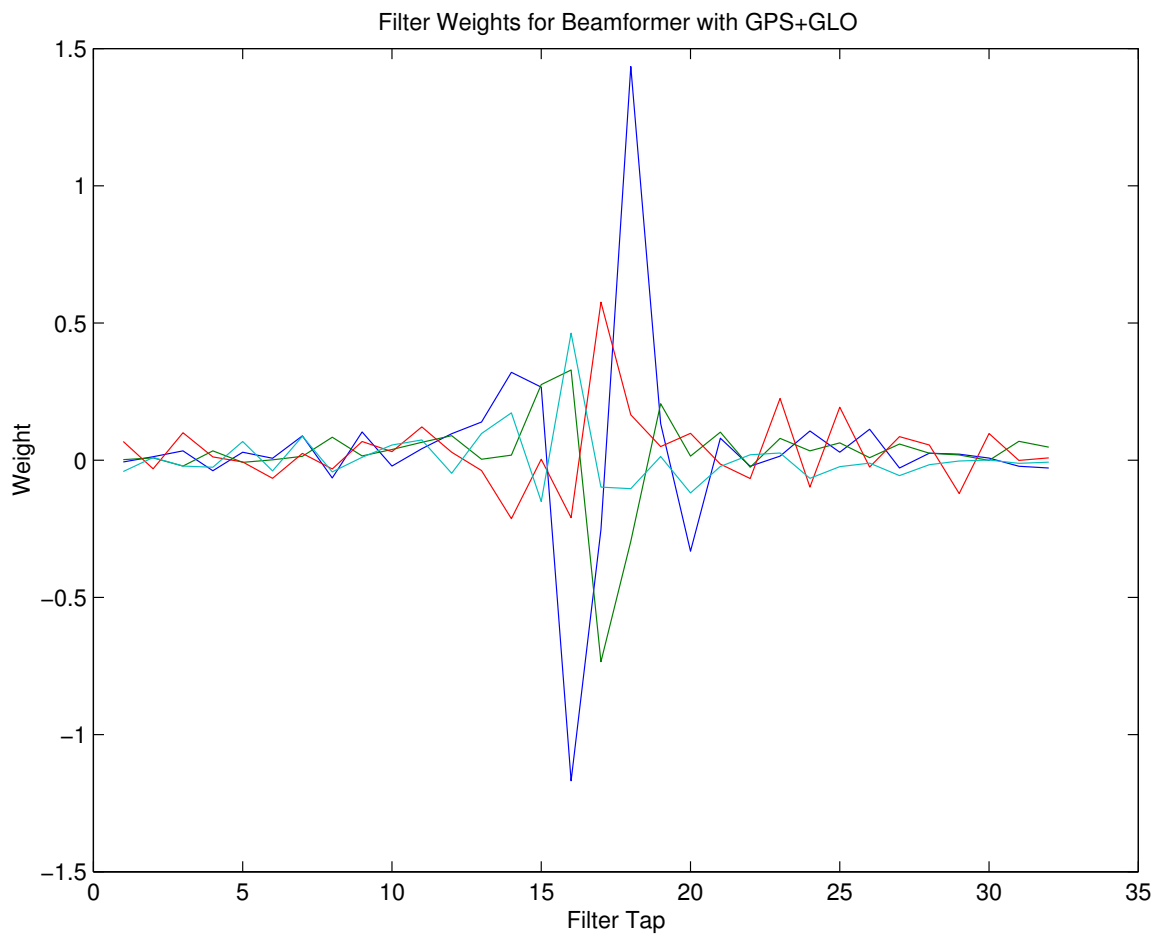


Fig. 7.— The rms as a function of integration time with successive application of Wiener filters to a simulated phased array signal containing GPS and Glonass data. Symbols are the same as in Figure 4, except that the noise data point is arbitrary and no single polarization solution is given.

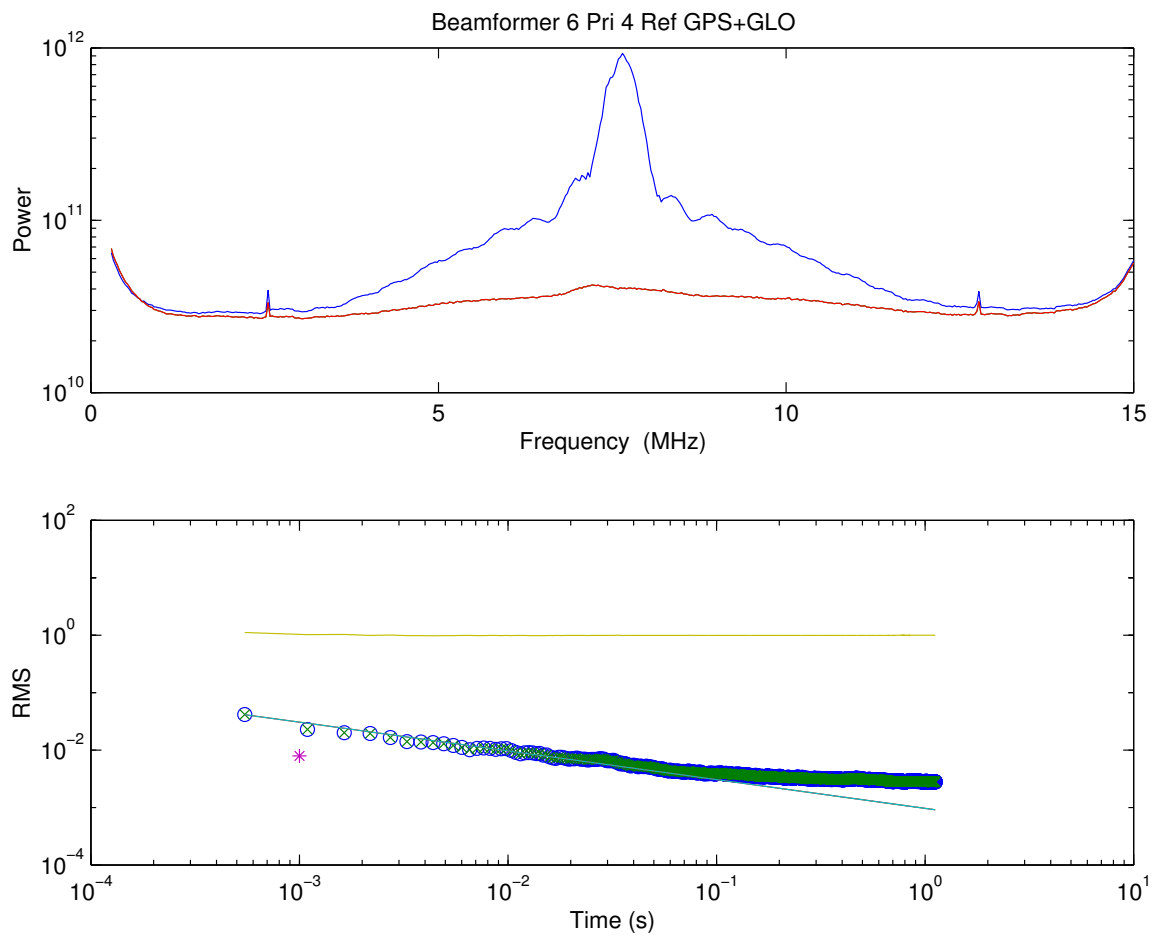


Fig. 8.— The rms as a function of integration time with successive application of Wiener filters to Glonass with (blue circles) and without (green crosses) update of the filter coefficients. Symbols are the same as in Figure 4

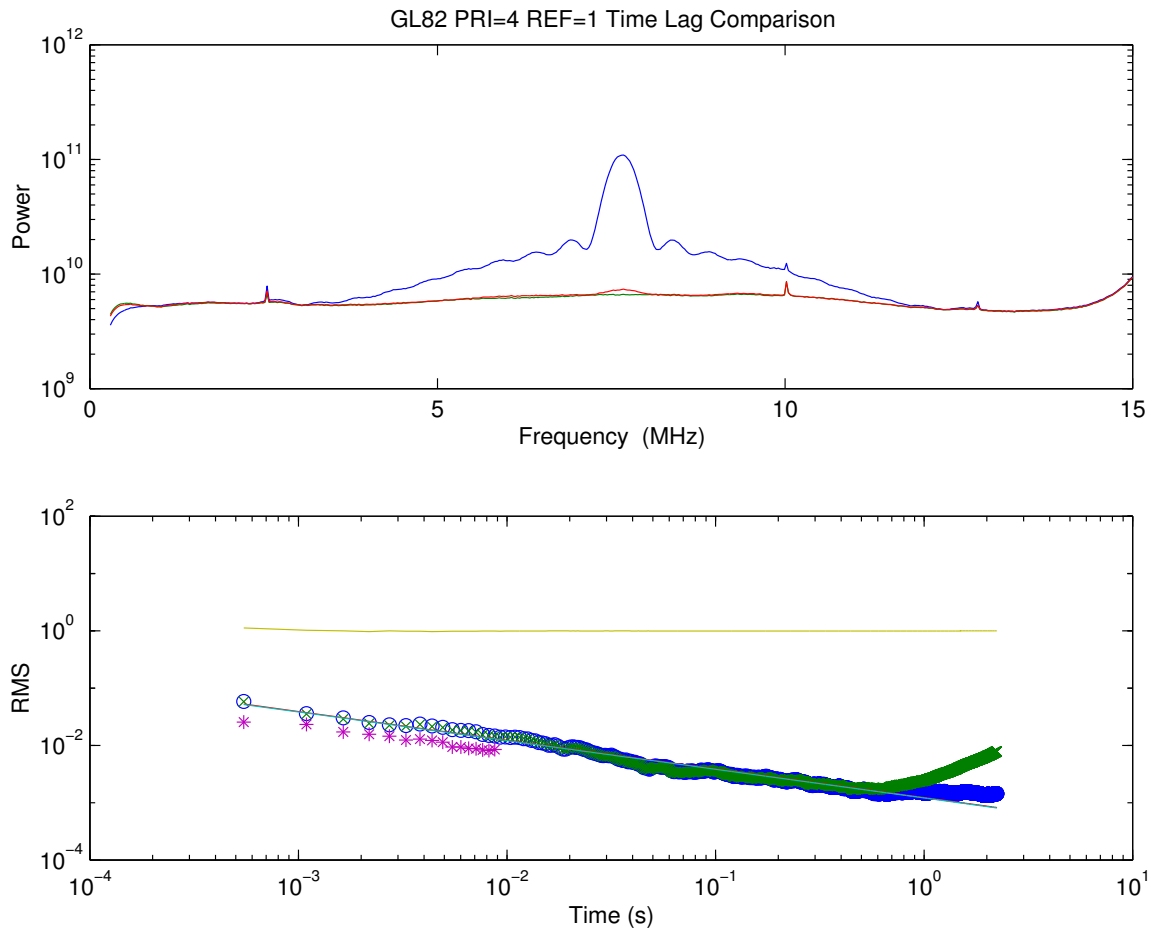


Fig. 9.— The rms as a function of integration time with successive application of Wiener filters to GPS with (blue circles) and without (green crosses) update of the filter coefficients. Symbols are the same as in Figure 4

